ACCOUNTS of chemical research

Article

pubs.acs.org/accounts

# Vacancy-Mediated Processes in the Oxidation of CO on PdO(101)

*Published as part of the Accounts of Chemical Research special issue "Microscopic Insights into Surface Catalyzed Chemical Reactions".*

Jason F. Weaver,*[,†] Feng Zhang,[†] Li Pan,[‡] Tao Li,[†] and Aravind Asthagiri[‡]

[†]Department of Chemical Engineering, University of Florida, Gainesville, Florida 32611, United States

[‡]William G. Lowrie Chemical & Biomolecular Engineering, The Ohio State University, Columbus, Ohio 43210, United States

**CONSPECTUS:** Metal oxide films can form on late transition-metal catalysts under sufficiently oxygen-rich conditions, and typically cause significant changes in the catalytic performance of these materials. Several investigations using sensitive in situ surface characterization techniques reveal that the CO oxidation activity of Pd and other late transition-metal catalysts increases abruptly under conditions at which metal oxide structures begin to develop. Findings such as these provide strong motivation for developing atomic-scale descriptions of oxidation catalysis over oxide films of the late transition-metals. Surface oxygen vacancies can play a central role in mediating oxidation catalysis promoted by metal oxides. In general, adsorbed reactants abstract oxygen atoms from the lattice of the oxide surface, thereby creating oxygen vacancies, while gaseous $O_2$ replenishes the reactive surface oxygen atoms and eliminates oxygen vacancies. Oxygen vacancies also represent a distinct type of surface site on which the binding and reactivity of adsorbed species can differ compared with sites on the pristine oxide surface. Detailed characterization of vacancy-mediated rate processes is thus essential for developing reliable mechanistic descriptions of oxidation catalysis over reducible metal oxide films. Careful measurements performed in ultrahigh vacuum (UHV) using well-defined oxide surfaces in combination with molecular simulations afford the capability to isolate and characterize such reaction steps, and thus provide information that is needed for developing mechanistic models of oxidation catalysis over metal oxides.

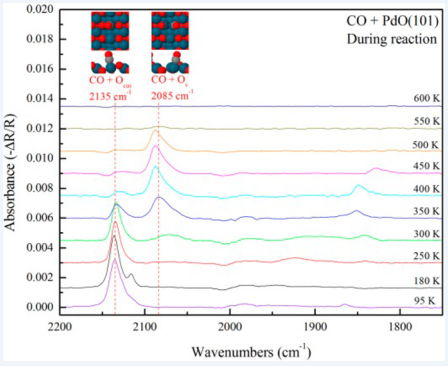


In this Account, we discuss vacancy-mediated processes that are involved in the oxidation of CO on the PdO(101) surface as determined from UHV surface science experiments and density functional theory (DFT) calculations. These studies show that CO binds strongly on Pd atoms that are located next to surface oxygen vacancies, and diffuses rapidly to these sites during reduction of the oxide surface by CO. The enhanced binding also raises the energy barriers for desorption and oxidation of CO, but the difference in these barriers remains nearly identical to that for CO adsorbed on the pristine PdO(101) surface. These recent studies also show that oxygen from the subsurface efficiently eliminates surface oxygen vacancies during CO oxidation at temperatures as low as 400 K, and thereby reveal a facile pathway by which PdO(101) surface domains can be maintained during oxide reduction.

## INTRODUCTION

The surface chemistry of late transition-metal oxides is fundamental to many applications of oxidation catalysis. Under oxygen-rich conditions, metal oxide layers can form on the surfaces of metallic catalysts and cause significant changes in catalyst performance because the surface chemical properties of metals and metal oxides are typically quite different. The importance of metal oxide films in the catalytic oxidation of CO has been widely discussed in the literature. This work has been motivated largely by in situ studies which show that late transition metals (Pd, Pt, Ru, Rh) tend to become highly active toward CO oxidation under conditions at which metal oxide structures begin to develop.[1−4] Of particular relevance to this Account are findings that a multilayer PdO(101) structure develops on crystalline Pd surfaces under catalytically relevant conditions, and that formation of the PdO(101) structure coincides with high catalytic activity for the oxidation of compounds such as CO and $CH_4$.[2,5,6] This finding suggests that fundamental investigations of PdO(101) surface chemistry can aid in advancing mechanistic descriptions of several Pd-catalyzed oxidation processes.

Oxidation catalysis over late transition-metal oxides typically involves oxygen exchange between the gaseous reactants and the oxide lattice, that is, the Mars van Krevelan mechanism. More specifically, adsorbed species abstract oxygen atoms from the surface lattice of the oxide while gaseous oxidants, usually $O_2$, regenerate the reactive surface oxygen atoms. Under steady-state reaction conditions, these processes work in tandem to both sustain the catalytic oxidation reaction and preserve the oxide structure. Oxygen vacancies play a central role in mediating catalysis by the Mars van Krevelan mechanism because such sites are created and eliminated in the catalytic cycle. Furthermore, oxygen vacancies represent a distinct type

**Received:** February 24, 2015
**Published:** May 1, 2015





DOI: 10.1021/acs.accounts.5b00101
*Acc. Chem. Res.* 2015, 48, 1515−1523

of surface site on which the binding and reactivity of adsorbed species may be modified relative to that on the pristine oxide surface. As such, oxygen vacancies can establish new kinetic pathways for the gaseous reactants, resulting in an intricate coupling between the reaction kinetics and the creation and annihilation of oxygen vacancies.

Researchers have extensively investigated CO oxidation on the $RuO_2(110)$ surface, and uncovered atomic-scale processes that govern this surface chemical reaction over a wide-range of conditions.[7,8] The stoichiometric $RuO_2(110)$ surface is comprised of rows of coordinatively unsaturated (cus) Ru atoms that are separated by rows of bridging O atoms ($O_{br}$). Vacancies can also exist in the bridging oxygen rows and the dissociation of $O_2$ can generate so-called on-top O atoms ($O_{ot}$) that bind on the $Ru_{cus}$ atoms. Prior studies demonstrate that CO molecules bind more strongly on bridging oxygen vacancies than on $Ru_{cus}$ atoms, and that $CO_{br}$ species can react with $O_{br}$ or $O_{ot}$ atoms by distinct pathways compared with $CO_{ot}$ species. Investigations using reflection absorption infrared spectroscopy (RAIRS) and kinetic Monte Carlo (kMC) have been particularly effective in revealing mechanistic aspects of CO oxidation on $RuO_2(110)$.[9,10] These studies indeed show that multiple local configurations can contribute to CO oxidation on $RuO_2(110)$, and that $CO_{br}$ species are particularly important under stoichiometric reaction conditions.

In this Account, we discuss vacancy-mediated processes involved in the oxidation of CO on the PdO(101) surface as determined by UHV surface science experiments in combination with density functional theory (DFT) calculations. These recent studies show that the creation of oxygen vacancies establishes new reaction pathways during CO oxidation on PdO(101), and reveal that lattice oxygen at the surface is efficiently regenerated by oxygen transport from the bulk reservoir. Our Account focuses on the identification of these vacancy-mediated processes, their influence on the CO oxidation kinetics and implications for developing microscopic descriptions of CO oxidation on PdO(101) under steady-state reaction conditions.

## DISCUSSION

### Preparation and Surface Structure of PdO(101)

We prepare PdO(101) films for surface science investigations in UHV by oxidizing Pd(111) with a plasma-generated O atom beam at a surface temperature of 500 K. The resulting PdO(101) film contains ~3 to 4 ML of O atoms and is highly crystalline with an atomically flat morphology.[11−13] The film thermally decomposes in UHV, giving rise to a sharp $O_2$ TPD peak centered at about 750 K that initiates near 650 K.

Figure 1 shows the structure of the stoichiometric PdO(101) surface that is the focus of our investigation. Bulk crystalline PdO has a tetragonal unit cell and consists of square planar units of Pd atoms 4-fold coordinated with oxygen atoms. The bulk-terminated PdO(101) surface is defined by a rectangular unit cell, where the *a* and *b* lattice vectors coincide with the [010] and [$\bar{1}$01] directions of the PdO crystal, respectively. The stoichiometric PdO(101) surface consists of alternating rows of 3-fold or 4-fold coordinated Pd or O atoms that run parallel to the *a* direction shown in Figure 1. Thus, half of the surface O and Pd atoms are coordinatively unsaturated (cus). The areal density of each type of coordinatively distinct atom of the PdO(101) surface is equal to 35% of the atomic density of the Pd(111) surface. Hence, the coverage of cus-Pd atoms is equal

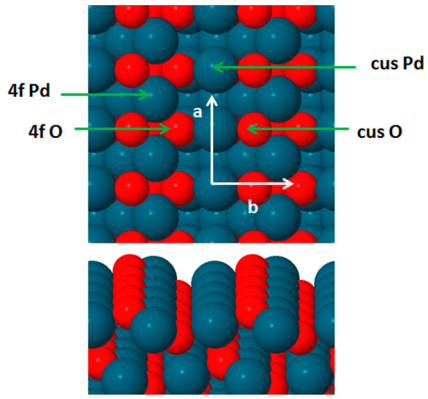


**Figure 1.** Top and side views of the PdO(101) surface. The red and dark blue atoms represent O and Pd atoms, respectively. Rows of coordinatively unsaturated (cus) and 4-fold-coordinated (4f) Pd or O atoms are indicated. The vertical and horizontal arrows a and b represent the [010] and [$\bar{1}$01] crystallographic directions of PdO.

to 0.35 ML, and each PdO(101) layer contains 0.7 ML of Pd atoms and 0.7 ML of O atoms.

### Creation of Surface Oxygen Vacancies during CO Oxidation on PdO(101)

Recent temperature-programmed reaction spectroscopy (TPRS) and RAIRS experiments in combination with DFT calculations provide new insights about the mechanism for CO oxidation on PdO(101), particularly the role of surface oxygen vacancies.[14] Figure 2 shows CO and $CO_2$ TPRS traces obtained

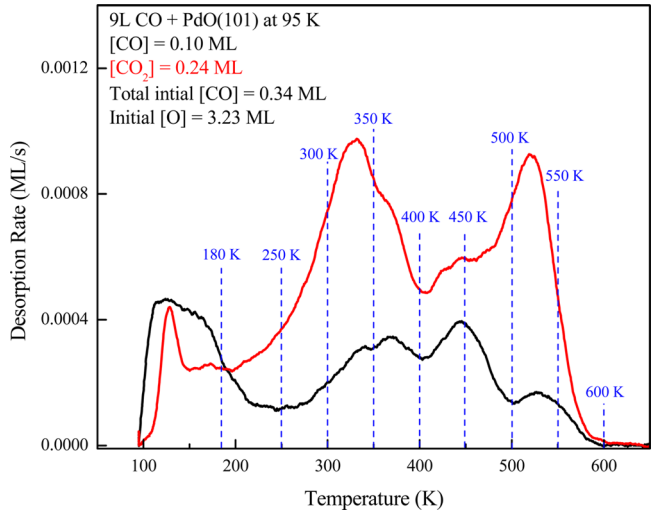


**Figure 2.** TPRS traces of CO (black) and $CO_2$ (red) obtained from a PdO(101) film after saturating with CO at 95 K.

after saturating a PdO(101) thin film with CO at 95 K. The results show that about 70% of the initially adsorbed CO oxidizes to $CO_2$ during the TPRS experiment, and thus reveal that CO oxidation is facile on PdO(101). The $CO_2$ TPRS trace exhibits a broad, complex shape that is characterized by two distinct maxima at 330 and 520 K. Approximately equal quantities of $CO_2$ desorb in the two TPRS features. The considerable breadth of the $CO_2$ TPRS trace indicates that CO oxidation on PdO(101) occurs by multiple rate processes during the TPRS experiment. This behavior is consistent with the idea that reduction of the PdO(101) surface by reaction


DOI: 10.1021/acs.accounts.5b00101
*Acc. Chem. Res.* 2015, 48, 1515−1523

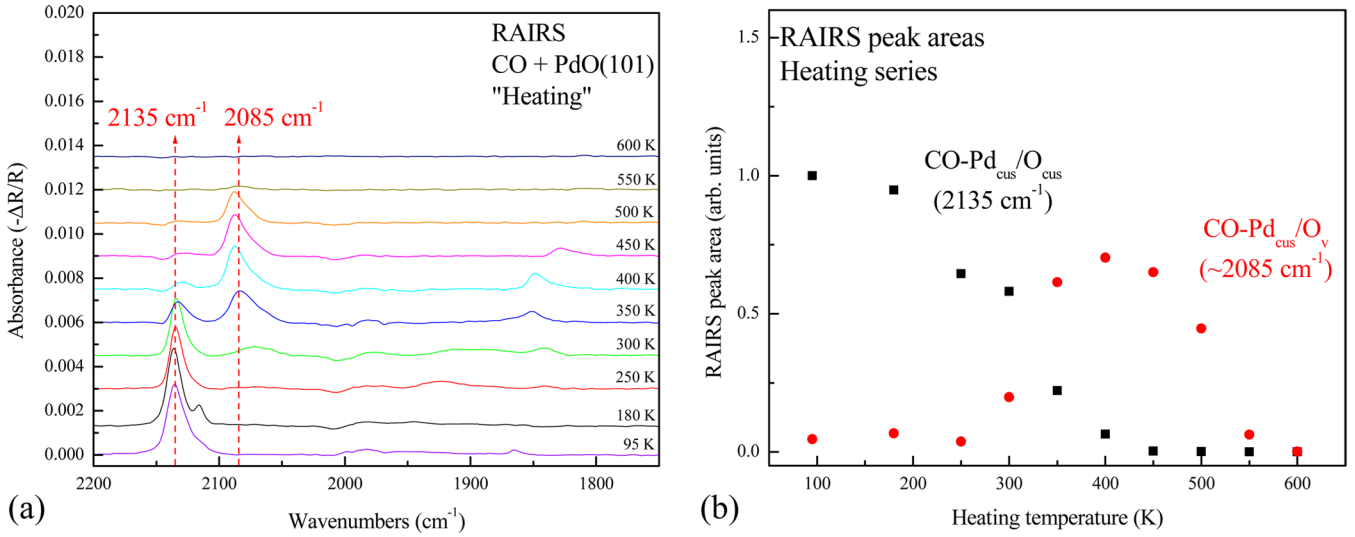


**Figure 3.** "Heating" series of RAIR spectra (a) and integrated area of atop CO peak at 2135 and 2085 $cm^{-1}$ as a function of heating temperature (b). Each RAIR spectrum was obtained at 95 K after heating CO-saturated PdO(101) to the temperatures indicated.

with CO creates new surface sites that modify the binding and reactivity of CO relative to that on the initial PdO(101) surface.

RAIRS measurements reveal that CO molecules preferentially bind on $O_{cus}$ vacancy ($O_v$) sites as these sites are created during surface reduction, and provide evidence that the low and high temperature $CO_2$ TPRS peaks originate from the oxidation of CO adsorbed on domains of the pristine PdO(101) surface versus CO adsorbed next to $O_v$ sites. Figure 3a shows a series of RAIRS spectra obtained after heating a saturated CO layer on PdO(101) to the temperatures indicated, followed by cooling to 95 K. Each spectrum was collected using a freshly prepared PdO(101) film and the initial CO layers were prepared at 95 K. This "heating" RAIRS series provides information about the surface binding sites occupied by CO during the TPRS experiment.

The RAIR spectrum obtained from the initial PdO(101) surface exhibits a dominant peak at 2135 $cm^{-1}$ that arises from CO adsorbed on top of $Pd_{cus}$ sites of PdO(101), that is, an atop-CO species, which we refer to as CO−$Pd_{cus}$/$O_{cus}$.[14,15] DFT calculations using the HSE functional[16] predict that CO strongly prefers to bind on atop-$Pd_{cus}$ sites rather than bridge-$Pd_{cus}$ sites, in agreement with the experimental RAIRS data.[14] It is worth noting that DFT-PBE predicts a negligible difference in the stability of CO adsorbed on atop-$Pd_{cus}$ versus bridge-$Pd_{cus}$ sites due primarily to the overestimation of back-donation contributions, but predicts a C−O stretching frequency of the atop CO−$Pd_{cus}$/$O_{cus}$ species that agrees well with the experimental value. The comparison of DFT vibrational frequencies and RAIRS spectra has been critical to identifying this fundamental issue with the DFT-PBE description of CO on PdO(101). In the heating RAIRS series, the intensity of the RAIRS peak at 2135 $cm^{-1}$ diminishes sharply and a new peak at ~2085 $cm^{-1}$ emerges as the temperature increases to values that pass through the first $CO_2$ TPRS peak (~300 to 400 K). Minor features also appear in the RAIR spectra at ~2115, 1983, and 1864 $cm^{-1}$ that are consistent with CO adsorbed on metallic Pd nanoclusters. The changes in these features with increasing temperature, particularly the diminution of the 2115 $cm^{-1}$ peak, likely indicate that Pd nanoclusters agglomerate into larger Pd(111) domains during the TPRS experiment.[14] Further increasing the temperature through the second $CO_2$ TPRS peak (~450−550 K) causes the RAIRS peak at 2085 $cm^{-1}$ to vanish in the "heating" series. Overall, the RAIRS data suggest that oxidation of the CO−$Pd_{cus}$/$O_{cus}$ species gives rise to the $CO_2$ TPRS peak at 330 K and reveal that a new type of adsorbed CO species concurrently forms and subsequently oxidizes to produce the $CO_2$ TPRS peak at 520 K.

DFT calculations provide strong evidence that the new RAIRS peak at 2085 $cm^{-1}$ arises from CO molecules that bind on atop-$Pd_{cus}$ sites located next to $O_v$ sites, which we refer to as CO−$Pd_{cus}$/$O_v$. First, DFT predicts that the C−O stretching frequency is red-shifted for the CO−$Pd_{cus}$/$O_v$ species compared with the CO−$Pd_{cus}$/$O_{cus}$ species, with values decreasing from 2109 to 2078 $cm^{-1}$ with increasing local CO coverage. The predicted redshift and the magnitude of the C−O stretching frequency of the CO−$Pd_{cus}$/$O_v$ species agree well with the experimental finding that a RAIRS peak emerges at ~2085 $cm^{-1}$ as CO oxidation initially reduces the PdO(101) surface during TPRS. Notably, Goodman and co-workers have also reported a C−O stretch peak near 2085 $cm^{-1}$ during PM-IRAS experiments of CO oxidation over crystalline Pd surfaces at high $O_2$/CO ratio and elevated pressure, supporting the idea that CO−$Pd_{cus}$/$O_v$ species on PdO(101) are prevalent under catalytically relevant conditions.[17] DFT calculations further predict that the CO binding energy is higher by ~70 kJ/mol for adsorption on a $Pd_{cus}$/$O_v$ site versus a $Pd_{cus}$/$O_{cus}$ site, which is generally attributable to the lower coordination number of the $Pd_{cus}$ atom of the $Pd_{cus}$/$O_v$ versus $Pd_{cus}$/$O_{cus}$ site (2-fold versus 3-fold). The strong binding provides an energetic driving force for CO molecules to diffuse to $Pd_{cus}$/$O_v$ sites as these sites are created during surface reduction. Lastly, DFT predicts that CO can diffuse rapidly along the $Pd_{cus}$ rows at the reaction temperatures (~ >300 K), with energy barriers for site hopping computed to be less than 40 kJ/mol. DFT calculations thus strongly support the idea that CO diffusion to $Pd_{cus}$/$O_v$ sites occurs in parallel with the desorption and oxidation of the CO−$Pd_{cus}$/$O_{cus}$ species during TPRS. The $Pd_{cus}$/$O_v$ sites effectively capture a large fraction of the CO molecules as $O_v$ sites are created during initial surface reduction.

DFT calculations also predict that both the CO−$Pd_{cus}$/$O_{cus}$ and CO−$Pd_{cus}$/$O_v$ species can access facile pathways for oxidation on PdO(101). Figure 4 shows the energy levels and


DOI: 10.1021/acs.accounts.5b00101
Acc. Chem. Res. 2015, 48, 1515−1523

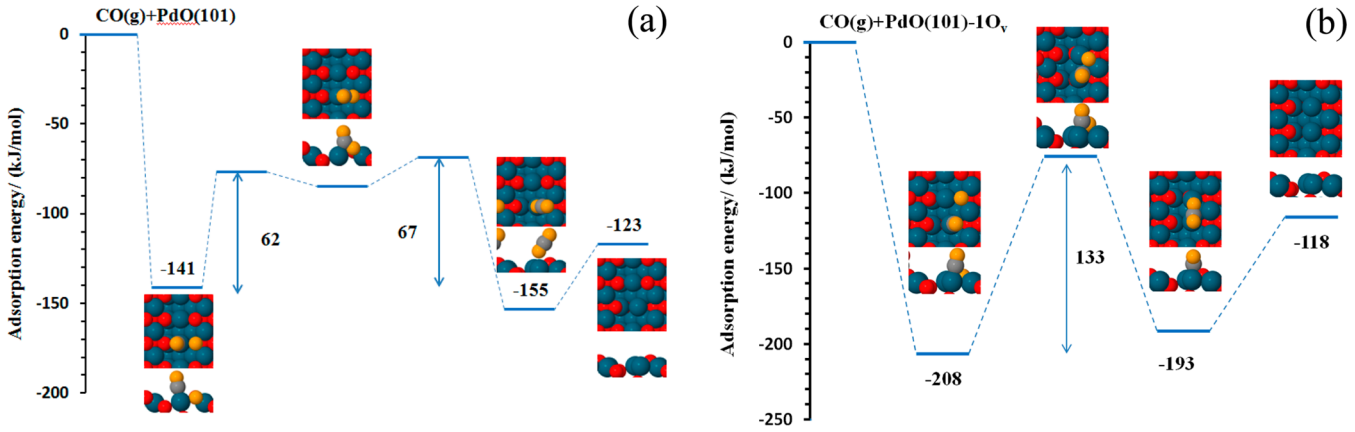


**Figure 4.** Computed energy diagrams for CO oxidation on pristine PdO(101) (a) and on PdO(101)−1O$_v$ (b).

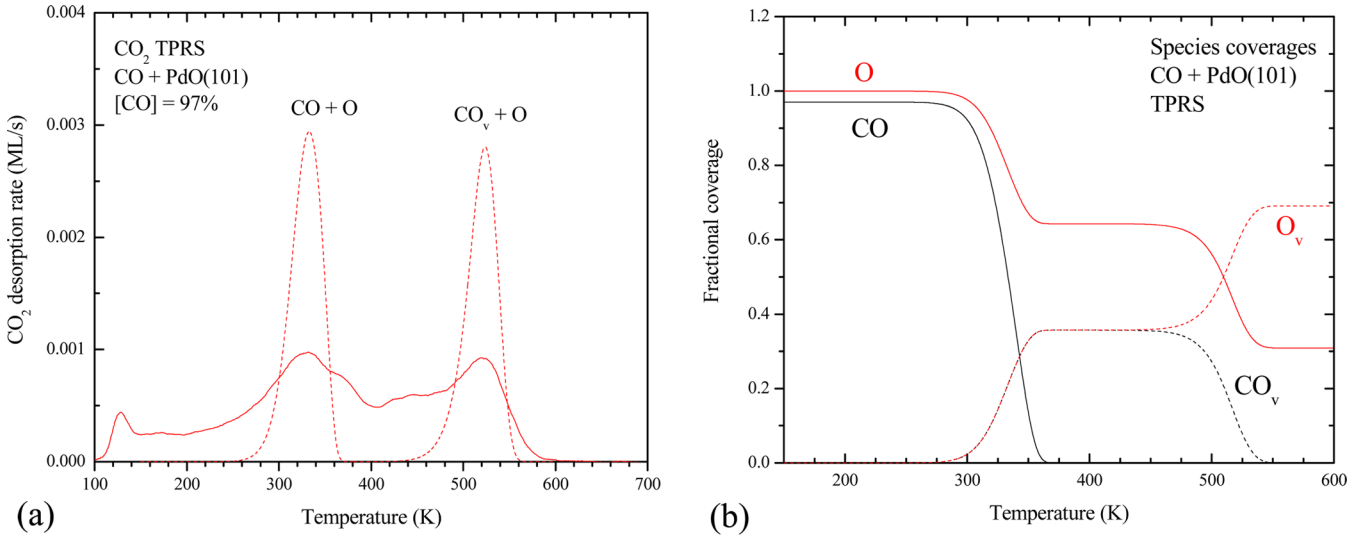


**Figure 5.** (a) $CO_2$ TPRS trace predicted (dashed line) using a mean-field kinetic model for an initial CO coverage of 97% compared with the experimental result (solid line) and (b) fractional coverages of CO, O, $CO_v$, and $O_v$ species as a function of the temperature during TPRS as predicted by the model.

images of the corresponding molecular structures for the computed reaction pathways. According to DFT, the CO−$Pd_{cus}/O_{cus}$ species oxidizes by abstracting the neighboring $O_{cus}$ atom to first form a $CO_2$-like intermediate which subsequently relaxes and desorbs, producing a gaseous $CO_2$ molecule and an $O_v$ site in the surface (Figure 4a). DFT-PBE calculations predict that the highest barrier relative to the initial adsorbed state of CO is 67 kJ/mol for this pathway, whereas the CO binding energy at the $Pd_{cus}/O_{cus}$ site is 141 kJ/mol. Thus, according to DFT, oxidation of the CO−$Pd_{cus}/O_{cus}$ species is energetically favored over desorption by a significant 74 kJ/mol and should occur readily, which is indeed consistent with our experimental finding that oxidation of the CO−$Pd_{cus}/O_{cus}$ species is facile and generates the low temperature $CO_2$ TPRS peak at ∼330 K.

Figure 4b depicts the computed pathway for oxidation of the CO−$Pd_{cus}/O_v$ species. In this pathway, the CO molecule abstracts an $O_{cus}$ atom that resides next to the adjacent $O_v$ site and produces a $CO_2$-like species which desorbs, thereby leaving a pair of $O_v$ sites on the surface. The energy barriers for desorption and oxidation of the CO−$Pd_{cus}/O_v$ species (208 and 133 kJ/mol) are both higher than those for the CO−$Pd_{cus}/O_{cus}$ species. However, the difference in these barriers is nearly identical for the CO−$Pd_{cus}/O_{cus}$ and CO−$Pd_{cus}/O_v$ species, with a value equal to ∼75 kJ/mol. The difference between the energy barrier for desorption ($E_d$) and reaction ($E_r$) of an adsorbed species is typically referred to as an apparent energy barrier for reaction ($E_r - E_d$) and represents the energy barrier for reaction measured relative to the gas-phase energy level. The larger barriers for desorption and oxidation of the CO−$Pd_{cus}/O_v$ species suggests that higher temperatures must be reached for the CO−$Pd_{cus}/O_v$ species to achieve comparable rates of reaction and desorption as the CO−$Pd_{cus}/O_{cus}$ species. Further, the similar values of the apparent reaction barriers suggests that the two CO species could experience similar branching between desorption and reaction during TPRS. These predictions agree well with the experimental findings that the desorption and reaction of the CO−$Pd_{cus}/O_v$ species produce the higher temperature desorption features during TPRS, and also that the $CO_2$ yields are nearly identical for the CO−$Pd_{cus}/O_{cus}$ and CO−$Pd_{cus}/O_v$ species.

## Simplified Kinetic Model for CO Oxidation on PdO(101)

A simplified kinetic model based on the mean-field approximation provides further insights for understanding how the creation of $O_v$ sites influences the kinetics of CO oxidation on PdO(101). Figure 5a shows $CO_2$ TPRS traces


DOI: 10.1021/acs.accounts.5b00101
Acc. Chem. Res. 2015, 48, 1515−1523

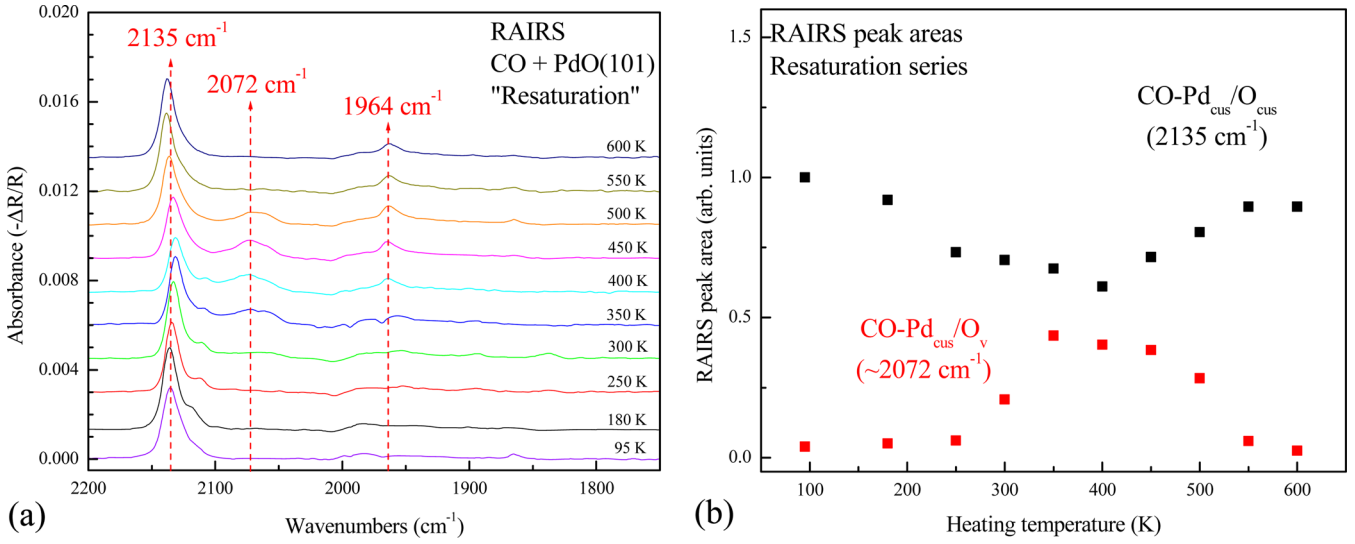


**Figure 6.** "Resaturation" series of RAIR spectra (a) and integrated area of atop CO peaks at 2135 and 2072 $cm^{-1}$ as a function of heating temperature (b). Each RAIR spectrum was obtained after heating CO-saturated PdO(101) to the temperatures indicated, followed by cooling and resaturating the surface with CO at 95 K.

predicted by the model and Figure 5b shows how species concentrations evolve with temperature during a TPRS experiment according to this model. The reaction steps included in the model may be represented by the following equations,

$$CO(g) \leftarrow CO + O_{cus} \rightarrow CO_2(g) + O_v$$

$$CO \rightarrow CO_v$$

$$CO(g) \leftarrow CO_v + O_{cus} \rightarrow CO_2(g) + 2O_v$$

where CO and $CO_v$ represent the $CO{-}Pd_{cus}/O_{cus}$ and $CO{-}Pd_{cus}/O_v$ species, respectively. The first and third equations represent the competing pathways for desorption and oxidation of the CO and $CO_v$ species, and the second equation represents the conversion of CO to $CO_v$ species via CO surface diffusion. The kinetic parameters used in the simulation were chosen to approximately reproduce the measured CO and $CO_2$ TPRS peak temperatures as well as the $CO_2$ yields in the low and high temperature desorption peaks.[14] We find that the rate of conversion of CO to $CO_v$ must be rapid to reproduce the nearly equal $CO_2$ desorption yields that emerge in the low versus high temperature TPRS peaks.

A key feature of the kinetic model is that the creation of $O_v$ sites establishes a new pathway for the CO species, namely, conversion to $CO_v$ species, that competes effectively with the desorption and reaction of CO. The model predicts that the concentration of CO species decreases rapidly to zero as the temperature increases through the first $CO_2$ TPRS peak and that the concentration of $CO_v$ species concurrently rises to a plateau (Figure 5b). According to the model, 36% of the initial CO species oxidizes to $CO_2$ and 36% converts to $CO_v$ species as $O_v$ sites are created by the reaction. As the temperature increases above ~460 K, oxidation of the $CO_v$ species produces the higher temperature $CO_2$ TPRS peak and the concentration of $CO_v$ species thus decreases to zero. We emphasize that the kinetic model fails to reproduce the detailed features observed in the experimental $CO_2$ (and CO) TPRS traces, which is expected. Processes such as the development of distinct types of local adlayer/surface configurations as well as reaction at metal-oxide domain boundaries might influence the CO oxidation kinetics and should be considered in future modeling.

The model illustrates how the migration of CO species to $Pd_{cus}/O_v$ sites generally influences the kinetics of CO oxidation on PdO(101) during TPRS. Specifically, the model shows that strong binding provides a driving force for CO molecules to diffuse to the $Pd_{cus}/O_v$ sites, and thereby establishes a reaction pathway that competes with desorption and oxidation of the $CO{-}Pd_{cus}/O_{cus}$ species and is also coupled to the reaction step since $O_v$ sites are created by CO oxidation. The conversion of CO to $CO_v$ species effectively delays the reaction and desorption of a large fraction of CO on PdO(101) to higher temperatures during TPRS.

## Regeneration of $O_{cus}$ Atoms

RAIRS measurements reveal that oxygen atoms from the bulk reservoir of PdO(101) regenerate surface $O_{cus}$ atoms and eliminate surface $O_v$ sites at temperatures above ~400 K during TPRS experiments of CO oxidation on the PdO(101) surface. Figure 6a shows RAIR spectra obtained after heating CO-saturated PdO(101) to the temperatures indicated, followed by cooling to 95 K and resaturating the surface with CO. This "resaturation" series of RAIRS data provides information about the binding sites that are present on the PdO(101) surface but not necessarily populated by CO during the TPRS experiment. A peak at 2135 $cm^{-1}$ is dominant in each of the resaturation RAIR spectra, demonstrating that $Pd_{cus}/O_{cus}$ sites are present in large concentrations on the PdO(101) surface throughout the TPRS experiment. A broad peak arising from $CO{-}Pd_{cus}/O_v$ species also becomes evident near ~2072 $cm^{-1}$ after heating to temperatures between ~300 and 500 K.

Figure 6b shows how the intensities of the peaks at 2135 and 2072 $cm^{-1}$ evolve with temperature in the resaturation RAIR spectra. Similar to the behavior observed in the heating RAIRS series (Figure 3), the intensity of the 2135 $cm^{-1}$ peak diminishes while that of the 2072 $cm^{-1}$ peak concurrently increases as the surface is heated to temperatures between ~300 and 500 K. Interestingly, the changes in the peak intensities reverse with continued heating above 500 K. The intensity of the 2072 $cm^{-1}$ peak diminishes sharply to zero with increasing temperature from ~450 to 600 K, while the intensity


DOI: 10.1021/acs.accounts.5b00101
Acc. Chem. Res. 2015, 48, 1515−1523

of the peak at 2135 $cm^{-1}$ increases, reaching a value that is nearly equal to that observed for CO adsorbed to saturation on clean PdO(101). This behavior demonstrates that surface $O_v$ sites are eliminated at temperatures above ~450 K during the TPRS experiment while $O_{cus}$ atoms are concurrently regenerated, even though oxidation of the CO−$Pd_{cus}$/$O_v$ species causes a net decrease in the O atom content of the PdO(101) film. A viable mechanism for this process is that O atoms from the subsurface fill surface $O_v$ sites, thereby regenerating $O_{cus}$ atoms.

DFT calculations support the idea that O atoms from the bulk reservoir regenerate surface $O_{cus}$ atoms during CO oxidation, and provide insights for understanding this process. An important finding from DFT is the prediction that surface $O_v$ sites are less stable than subsurface oxygen vacancies in PdO(101) but that the CO−$Pd_{cus}$/$O_v$ species stabilizes surface $O_v$ sites. According to DFT, the energy required to remove an $O_{cus}$ atom from PdO(101) is about 55 kJ/mol higher than that needed to remove an O atom that bonds to a $Pd_{cus}$ atom on the underside of the first PdO(101) layer, that is, a subsurface O atom (Figure 7). This prediction suggests that the PdO(101)

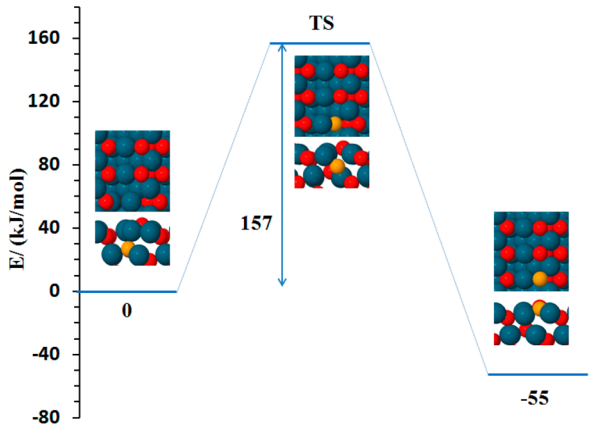


**Figure 7.** Pathway identified by DFT for the conversion of a subsurface O atom to an $O_{cus}$ atom on PdO(101) via filling of a surface $O_v$ site.

structure will be stabilized if a surface $O_v$ site is filled by a subsurface O atom. However, DFT also predicts that the formation energy of a surface $O_v$ site is ~96 kJ/mol lower than that of a subsurface $O_v$ site when a CO molecule is adsorbed on the adjacent $Pd_{cus}$ atom, thus demonstrating that adsorbed CO significantly stabilizes surface $O_v$ sites on PdO(101).

DFT also predicts a relatively facile pathway by which a subsurface O atom shifts into a surface $O_v$ site to regenerate an $O_{cus}$ atom and create a subsurface $O_v$ site in PdO(101) as shown in Figure 7. The computed pathway features an energy barrier of 157 kJ/mol, based on DFT-PBE calculations, and involves a rotation of the subsurface O atom (yellow) about the $Pd_{cus}$ atom that moves the O atom into the surface $O_v$ site, and thus restores an $O_{cus}$ atom in the surface. The predicted energy barrier for this pathway (157 kJ/mol) is rather moderate and lies between the values determined for the desorption and oxidation of the CO−$Pd_{cus}$/$O_v$ species (208 and 133 kJ/mol). The relative values of the energy barriers suggest that the regeneration of $O_{cus}$ atoms via subsurface O atoms could indeed occur at rates that are comparable to those at which CO vacates $Pd_{cus}$/$O_v$ sites during TPRS, which is consistent with experimental observations.

## Isothermal CO Oxidation

Direct rate measurements demonstrate that the creation and elimination of surface $O_v$ sites play critical roles in promoting and sustaining CO oxidation on PdO(101) under isothermal conditions.[18] Figure 8 shows the rate of $CO_2$ production measured as a function of time for the oxidation of CO on PdO(101) at constant temperatures of 350 and 450 K. In these experiments, a PdO(101) film containing ~3.5 ML of oxygen atoms is maintained at constant temperature and the CO partial pressure is abruptly increased to $5 \times 10^{-9}$ Torr at the start of the measurement. Simultaneous monitoring of the $CO_2$ partial pressure provides a direct measure of the $CO_2$ production rate as CO oxidation reduces the PdO(101) film. The experiment is terminated once the $CO_2$ partial pressure returns to the initial baseline, signaling that reaction with CO has ceased.

The isothermal data reveals a marked difference in the CO oxidation behavior for surface temperatures above versus below ~400 K. First, the reaction kinetics becomes self-accelerating at $T \sim >400$ K in that the rate of $CO_2$ production increases steadily as the PdO(101) film is consumed by reaction, reaching a maximum near the end of the isothermal experiment. Furthermore, the total $CO_2$ yield obtained in the experiments exhibits a dramatic increase when reaction is conducted at temperatures of 400 K and higher. At 350 K, CO oxidation effectively ceases once the reaction consumes about 0.66 ML of O atoms from the oxide (Figure 8a), which corresponds closely to the quantity of oxygen in one layer of PdO(101). In contrast, CO oxidation completely reduces the 3.5 ML PdO(101) film at temperatures ~ >400 K.

RAIRS measurements reveal significant differences in the surface structure when CO oxidation occurs at temperatures at which the PdO(101) film undergoes partial versus complete reduction. RAIR spectra show that CO molecules bind mainly to $Pd_{cus}$/$O_v$ sites during isothermal reaction at temperatures above 400 K, and that both $Pd_{cus}$/$O_{cus}$ and $Pd_{cus}$/$O_v$ sites are present on the surface throughout the self-accelerating kinetic regime (Figure 8b), even after as much as 3 ML of O atoms are removed from the film.[18] These observations provide strong evidence that the regeneration of $O_{cus}$ atoms via subsurface oxygen migration maintains surface PdO(101) domains during isothermal CO oxidation above 400 K, and that the coexistence of $O_{cus}$ and $O_v$ sites at the surface promotes reaction.

For comparison, RAIRS reveals that PdO(101) surface domains are present only in small quantities after the CO oxidation rate diminishes at 350 K and that metallic Pd nanoclusters are the dominant surface structure (Figure 8b). This behavior suggests that the regeneration of $O_{cus}$ sites is too slow to sustain PdO(101) surface domains during CO oxidation at 350 K in the absence of gaseous $O_2$, and that surface $O_v$ sites created by CO oxidation instead agglomerate to produce small metallic domains.

The overall picture that emerges from isothermal measurements is that both $O_{cus}$ and $O_v$ sites are needed to sustain CO oxidation on PdO(101), and that regeneration of the $O_{cus}$ atoms via oxygen transport from the bulk reservoir occurs efficiently above temperatures of ~400 K. Surface $O_v$ sites play a critical role in maintaining the high reactivity of the PdO(101) film. First, the facile migration of CO from $Pd_{cus}$/$O_{cus}$ to $Pd_{cus}$/$O_v$ sites represents a pathway that competes with reaction of the CO−$Pd_{cus}$/$O_{cus}$ species, and thus lowers the reaction probability of the CO−$Pd_{cus}$/$O_{cus}$ species as $O_v$ sites are created. The observation of self-accelerating kinetics further suggests that the branching probability for reaction of the $CO_v$


DOI: 10.1021/acs.accounts.5b00101
Acc. Chem. Res. 2015, 48, 1515−1523

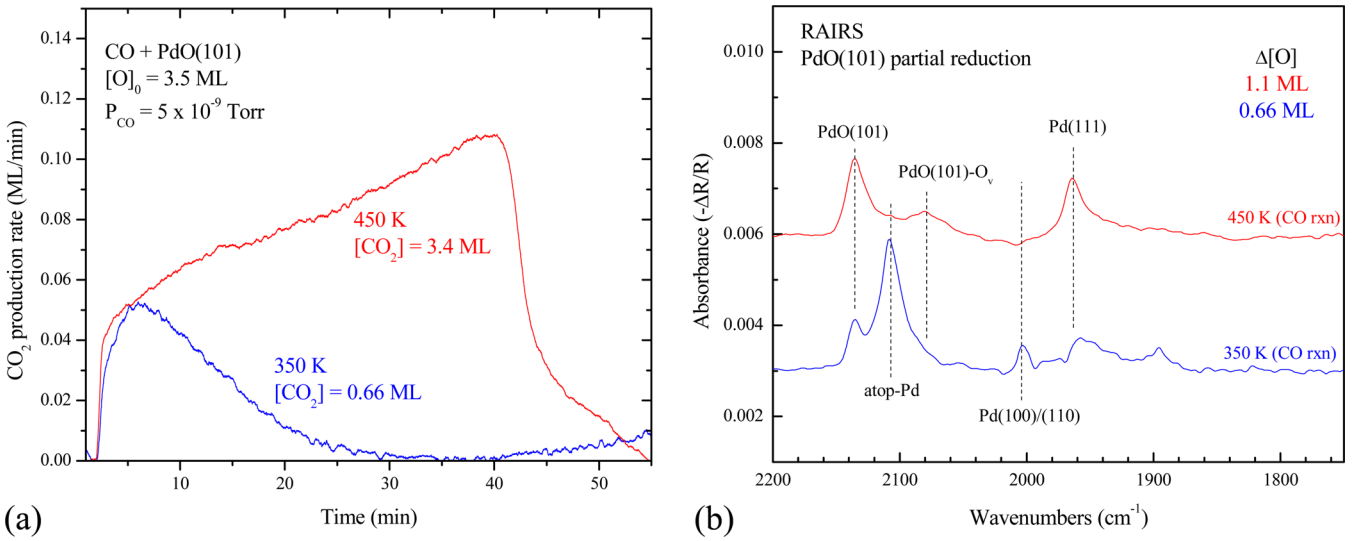


**Figure 8.** (a) Isothermal CO oxidation rate on a 3.5 ML PdO(101) film at 350 and 450 K in $5 \times 10^{-9}$ Torr of CO. (b) Resaturation CO RAIR spectra obtained after removal of 0.66 and 1.1 ML of O atoms from the PdO(101) film by CO oxidation at 350 and 450 K, respectively. After partial reduction, each surface was saturated with CO at 95 K prior to collecting the RAIRS data.

species is higher than that of the CO species at $T \sim$ >400 K. In this case, the reaction rate increases because the creation of $O_v$ sites is accompanied by an increase in the coverage of $CO_v$ species. Lastly, since $O_{cus}$ atoms are efficiently regenerated from the bulk reservoir only at temperatures $\sim$ >400 K, the strong binding and favorable reactivity of the CO−$Pd_{cus}/O_v$ species is also critical to allowing reduction of the PdO(101) film to go to completion.

## CONNECTIONS TO STEADY-STATE CO OXIDATION

We have uncovered new mechanistic details about CO oxidation on PdO(101) films through the combined use of surface science experiments and DFT calculations, finding that oxygen vacancies play a central role in mediating this chemistry. While these details aid in developing a kinetic description of CO oxidation on PdO(101), several issues must be addressed to describe this reaction at catalytically relevant pressures and steady-state conditions. A critical issue is determining reaction steps that govern the regeneration of PdO(101) domains or sites via the dissociation of $O_2$. Indeed, oxygen supplied from the gas-phase is needed to maintain the PdO(101) layer during steady-state CO oxidation by the Mars van Krevelan mechanism because CO reacts with lattice oxygen atoms at the oxide surface and the lattice oxygen is ultimately restored by $O_2$ in the gas-phase.

Prior investigations show that $O_2$ dissociation is unfavorable on the $Pd_{cus}$ row of pristine PdO(101) but that dissociation should be facile at $Pd_{cus}/O_v$ sites of PdO(101). An experimental investigation reported Hinojosa et al.[19] shows that $O_2$ molecules bind relatively strongly on PdO(101) but that dissociation occurs to a negligible extent during TPD. Consistent with this finding, DFT studies reveal that $O_2$ dissociation on stoichiometric PdO(101) is energetically unfavorable because the product of $O_2$ dissociation, a pair of O atoms chemisorbed on $Pd_{cus}$ sites, is less stable than $O_2$ adsorbed in molecular form on PdO(101).[8,20] In contrast, a DFT study by Hirvi et al.[20] reports a pathway for $O_2$ dissociation at a surface $O_v$ site featuring an energy barrier between only 50 and 55 kJ/mol, suggesting that regeneration of $O_{cus}$ atoms via $O_2$ dissociation is intrinsically facile. These prior studies also suggest that direct reaction between coadsorbed $O_2$ and CO molecules is a viable pathway for CO oxidation on PdO(101).[19,20] The extent to which such processes participate in steady-state CO oxidation requires further study.

The importance of more reduced structures in CO oxidation on PdO(101) films needs to be further addressed as well. For example, our RAIRS studies show that CO oxidation on PdO(101) produces metallic Pd domains on which CO adsorbs during TPRS and isothermal experiments.[14,18] Reaction with oxygen adsorbed on the metal domains or at oxide-metal domain boundaries can contribute to the reaction rate on PdO(101), and is particularly important in CO oxidation on 2D oxide structures.[18,21] STM experiments also reveal that the thermal decomposition of PdO(101) films at temperatures above 700 K produces distinct surface structures.[13] Such findings highlight the need to further investigate the dynamic coupling between the surface structure and chemical reactivity of PdO(101) films over a wide range of conditions.

## SUMMARY AND OUTLOOK

Recent studies show that surface oxygen vacancies play a central role in mediating the oxidation of CO on the PdO(101) surface. This work shows that enhanced binding at $Pd_{cus}/O_v$ sites as well as fast CO diffusion cause CO species to rapidly convert to $CO_v$ species during CO oxidation on PdO(101), and that this conversion process competes effectively with the desorption and oxidation of CO adsorbed on $Pd_{cus}/O_{cus}$ sites. The strong binding of the CO−$Pd_{cus}/O_v$ species also raises the absolute energy barriers for desorption and oxidation of the $CO_v$ versus CO species, but the apparent barriers for reaction remain nearly identical for the two species. As a result, the $CO_v$ species require higher temperatures to react at comparable rates as the CO species, but the branching probabilities for oxidation of the CO versus $CO_v$ species are similar though offset as a function of the surface temperature. The work further reveals that oxygen from the subsurface efficiently regenerates surface $O_{cus}$ atoms on PdO(101) after CO vacates $Pd_{cus}/O_v$ sites. This regeneration process together with the strong binding and high reactivity of the $CO_v$ species enables CO to completely reduce PdO(101) thin films at temperatures as low as 400 K.



DOI: 10.1021/acs.accounts.5b00101
Acc. Chem. Res. 2015, 48, 1515−1523

These recent studies demonstrate that careful UHV experiments in combination with DFT calculations are essential for uncovering atomic-scale processes involved in the oxidation of CO on PdO(101) and ultimately providing information needed to develop accurate kinetic models of this reaction. However, several other molecular processes require clarification before reliable models can be developed to describe CO oxidation on PdO(101) under steady-state conditions. Examples include the mechanisms by which gaseous $O_2$ restores $O_{cus}$ atoms on PdO(101), the importance of direct reactions between adsorbed CO and $O_2$ and the possible role of more complex, reduced structures that may coexist with PdO(101) surface domains. Accurately characterizing such processes at the atomic scale and identifying their importance over a wide range of steady-state reaction conditions will require a combination of UHV experiments, DFT calculations, and in situ measurements.

## AUTHOR INFORMATION


### Corresponding Author

*E-mail: weaver@che.ufl.edu. Telephone: 352-392-0869. Fax: 352-392-9513.


### Notes

The authors declare no competing financial interest.

### Biographies

**Jason F. Weaver** obtained his B.S. in Chemical Engineering at the University of Florida in 1992 and his Ph.D. from Stanford University in 1998 with Prof. Robert J. Madix. He joined the faculty of the Department of Chemical Engineering at the University of Florida in 1999 where he is currently the Charles Stokes Professor of Chemical Engineering.

**Feng Zhang** obtained his B.S. in Materials Science from Beijing Institute of Technology in 2009 and is currently a doctoral student in Chemical Engineering at the University of Florida with Prof. Jason F. Weaver.

**Li Pan** obtained his B.S. in Chemical Engineering from Beijing University of Chemical Technology in 2009 and is currently a doctoral student in Chemical & Biomolecular Engineering at the Ohio State University with Prof. Aravind Asthagiri.

**Tao Li** obtained her B.S. in Chemical Engineering from Jilin University in 2012 and is currently a doctoral student in Chemical Engineering at the University of Florida with Prof. Jason F. Weaver.

**Aravind Asthagiri** obtained his B.S. in Chemical Engineering from The Ohio State University in 1998 and his Ph.D. from Carnegie Mellon University in 2003 with Prof. David S. Sholl. He was an Assistant Professor at the University of Florida from 2005-2010, and has been an Associate Professor at The Ohio State University since 2010.

## ACKNOWLEDGMENTS

We acknowledge the Ohio Supercomputing Center for providing computational resources. We gratefully acknowledge financial support for this work provided by the Department of Energy, Office of Basic Energy Sciences, Catalysis Science Division through Grant DE-FG02-03ER15478.

## REFERENCES


(1) Gao, F.; McClure, S. M.; Cai, Y.; Gath, K. K.; Wang, Y.; Chen, M. S.; Guo, Q. L.; Goodman, D. W. CO oxidation trends on Pt-group metals from ultrahigh vacuum to near atmospheric pressures: A combined in situ PM-IRAS and reaction kinetics study. *Surf. Sci.* **2009**, *603*, 65−70.

(2) van Rijn, R.; Balmes, O.; Resta, A.; Wermeille, D.; Westerstrom, R.; Gustafson, J.; Felici, R.; Lundgren, E.; Frenken, J. W. M. Surface structure and reactivity of Pd(100) during CO oxidation near ambient pressures. *Phys. Chem. Chem. Phys.* **2011**, *13*, 13167−13171.

(3) Hendriksen, B. L. M.; Frenken, J. W. M. CO oxidation on Pt(110): Scanning tunneling microscopy inside a high-pressure flow reactor. *Phys. Rev. Lett.* **2002**, *89*, 046101.

(4) Gustafson, J.; Westerstroem, R.; Mikkelsen, A.; Torrelles, X.; Balmes, O.; Bovet, N.; Andersen, J. N.; Baddeley, C. J.; Lundgren, E. Sensitivity of catalysis to surface structure: The example of CO oxidation on Rh under realistic conditions. *Phys. Rev. B* **2008**, *78*, 045423.

(5) Martin, N. M.; van den Bossche, M.; Hellman, A.; Gronbeck, H.; Hakanoglu, C.; Gustafson, J.; Blomberg, S.; Johanson, N.; Liu, Z.; Axnanda, S.; Weaver, J. F.; Lundgren, E. Intrinsic ligand effect governing the catalytic activity of Pd oxide thin films. *ACS Catal.* **2014**, *4*, 3330−3334.

(6) Hellman, A.; Resta, A.; Martin, N. M.; Gustafson, J.; Trinchero, A.; Carlsson, P. A.; Balmes, O.; Felici, R.; van Rijn, R.; Frenken, J. W. M.; Andersen, J. N.; Lundgren, E.; Gronbeck, H. The Active Phase of Palladium during Methane Oxidation. *J. Phys. Chem. Lett.* **2012**, *3*, 678−682.

(7) Over, H. Surface Chemistry of Ruthenium Dioxide in Heterogeneous Catalysis and Electrocatalysis: From Fundamental to Applied Research. *Chem. Rev.* **2012**, *112*, 3356−3426.

(8) Weaver, J. F. Surface Chemistry of Late Transition Metal Oxides. *Chem. Rev.* **2013**, *113*, 4164−4215.

(9) Farkas, A.; Hess, F.; Over, H. Experiment-Based Kinetic Monte Carlo Simulations: CO Oxidation over RuO2(110). *J. Phys. Chem. C* **2012**, *116*, 581−591.

(10) Farkas, A.; Mellau, G. C.; Over, H. Novel Insight in the CO Oxidation on RuO2(110) by in Situ Reflection-Absorption Infrared Spectroscopy. *J. Phys. Chem. C* **2009**, *113*, 14341−14355.

(11) Kan, H. H.; Weaver, J. F. A PdO(101) thin film grown on Pd(111) in ultrahigh vacuum. *Surf. Sci.* **2008**, *602*, L53−L57.

(12) Kan, H. H.; Weaver, J. F. Mechanism of PdO thin film formation during the oxidation of Pd(111). *Surf. Sci.* **2009**, *603*, 2671−2682.

(13) Hinojosa, J. A.; Weaver, J. F. Surface structural evolution during the thermal decomposition of a PdO(101) thin film. *Surf. Sci.* **2011**, *605*, 1797−1806.

(14) Zhang, F.; Pan, L.; Li, T.; Diulus, J.; Asthagiri, A.; Weaver, J. F. CO oxidation on PdO(101) during temperature programmed reaction spectroscopy: Role of oxygen vacancies. *J. Phys. Chem. C* **2014**, *118*, 28647−28661.

(15) Martin, N. M.; Van den Bossche, M.; Gronbeck, H.; Hakanoglu, C.; Zhang, F.; Li, T.; Gustafson, J.; Weaver, J. F.; Lundgren, E. CO Adsorption on Clean and Oxidized Pd(111). *J. Phys. Chem. C* **2014**, *118*, 1118−1128.

(16) Heyd, J.; Scuseria, G. E.; Ernzerhof, M. Hybrid Functionals based on a Screened Coulomb Potential. *J. Chem. Phys.* **2003**, *118*, 8207−8215.

(17) Gao, F.; Wang, Y.; Cai, Y.; Goodman, D. W. CO Oxidation on Pt-Group Metals from Ultrahigh Vacuum to Near Atmospheric Pressures. 2. Palladium and Platinum. *J. Phys. Chem. C* **2009**, *113*, 174−181.

(18) Zhang, F.; Li, T.; Pan, L.; Asthagiri, A.; Weaver, J. F. CO oxidation on single and multilayer Pd oxides on Pd(111): Mechanistic insights from RAIRS. *Catal. Sci. Technol.* **2014**, *4*, 3826−3834.

(19) Hinojosa, J. A.; Kan, H. H.; Weaver, J. F. Molecular chemisorption of $O_2$ on a PdO(101) thin film on Pd(111). *J. Phys. Chem. C* **2008**, *112*, 8324−8331.

(20) Hirvi, J. T.; Kinnunen, T. J. J.; Suvanto, M.; Pakkanen, T. A.; Norskov, J. K. CO oxidation on PdO surfaces. *J. Chem. Phys.* **2010**, *133*, 084704.




DOI: 10.1021/acs.accounts.5b00101
*Acc. Chem. Res.* 2015, 48, 1515−1523

(21) Hoffmann, M. J.; Reuter, K. CO Oxidation on Pd(100) Versus PdO(101)-($\sqrt{5} \times \sqrt{5}$)R27°: First-Principles Kinetic Phase Diagrams and Bistability Conditions. *Top. Catal.* **2014**, *57*, 159−170.



DOI: 10.1021/acs.accounts.5b00101
*Acc. Chem. Res.* 2015, 48, 1515−1523